OFFICE OF NAVAL RESEARCH

Technical Report #7

"Crystal Structure, Reactivity, and Photochemical Properties of the Tungsten(0) Zwitterionic Amido Complex (CO)5WNPhNPhC(OMe)Ph."

by

Scott T. Massey, Nicholas D.R. Barnett, Khalil A. Abboud and Lisa McElwee-White*

DTIC QUALITY INSPECTED 4

May 14, 1996

19960531 066

REPORT DOCUMENTATION PAGE

Public reporting burden for this collection of information is estimated to average 1 hour per response, including the time for reviewing instructions, searching existing data sour gathering and maintaining the data needed, and completing and reviewing the collection of information. Send comments regarding this burden estimate or any other aspect of collection of information, including suggestions for reducing this burden, to Washington Headquarters Services, Directorate for Information Operations and Reports, 1215 Jeffer Davis Highway, Suite 1204, Arlington, VA 22202-4302, and to the Office of Management and Budget, Paperwork Reduction Project (0704-0188), Washington, DC 20503.

1. AGENCY USE ONLY (Leave blank)	2. REPORT DATE 5/14/96	3. REPORT TYPE AND DATES COVERED Technical

4. TITLE AND SUBTITLE
Crystal Structure, Reactivity, and Photochemical Properties of Tungsten(0) Zwitterionic Amido Complex $(CO)_5WNPhNPhC(OMe)Ph$

5. FUNDING NUMBERS
N0014-95-1-0563
R&T Code: 3135027
Dr. Harold E. Guard

6. AUTHOR(S)
Scott T. Massey, Nicholas D. R. Barnett, Khalil A. Abboud and Lisa McElwee-White*

7. PERFORMING ORGANIZATION NAME(S) AND ADDRESS(ES)
Department of Chemistry
University of Florida
Gainesville, FL 32611-7200

8. PERFORMING ORGANIZATION REPORT NUMBER
Technical Report #7

9. SPONSORING/MONITORING AGENCY NAME(S) AND ADDRESS(ES)
Office of Naval Research
Ballston Tower One
800 N. Quincy St.
Arlington, VA 22217-5000

10. SPONSORING/MONITORING AGENCY REPORT NUMBER

11. SUPPLEMENTARY NOTES

12a. DISTRIBUTION/AVAILABILITY STATEMENT
Reproduction in whole or in part is permitted for any purpose of the United States Government. This document has been approved for public release and sale; its distribution is unlimited.

12b. DISTRIBUTION CODE

13. ABSTRACT (Maximum 200 words)

The crystal structure of the zwitterionic complex $(CO)_5WNPhNPhC(Ph)OMe$ (**1**) shows that it is best described as an amido complex in which the "imidate" fragment $PhN=C(Ph)OMe$ serves as a substituent on the amide nitrogen. The structural information allows the previously reported conversion of **1** to an isomeric zwitterion to be assigned as simple rotation about the N-C double bond. The twisted intermediate for such a rotation also offers a pathway for the previously reported isomerization of **1** to a 2,4-diazametallacycle. The electronic spectrum of **1** reveals a low energy MLCT transition that is responsible for its photodecomposition via N-N bond cleavage. INDO/1 CI calculations support assignment of the MLCT band as the HOMO to LUMO transition, where depopulation of the HOMO initiates the cleavage of the N-N bond.

14. SUBJECT TERMS			15. NUMBER OF PAGES 29
amido complex, zwitterion, crystal structure			16. PRICE CODE

17. SECURITY CLASSIFICATION OF REPORT	18. SECURITY CLASSIFICATION OF THIS PAGE	19. SECURITY CLASSIFICATION OF ABSTRACT	20. LIMITATION OF ABSTR
unclassified	unclassified	unclassified	

NSN 7540-01-280-5500

Standard Form 298 (Rev. 2-8
Prescribed by ANSI Std. 239-18
298-102

DISCLAIMER NOTICE

UNCLASSIFIED

Technical Report
distributed by

**DEFENSE
TECHNICAL
INFORMATION
CENTER**

DTIC Acquiring Information-
Reporting Knowledge

Cameron Station
Alexandria, Virginia 22304-6145

UNCLASSIFIED

THIS DOCUMENT IS BEST
QUALITY AVAILABLE. THE
COPY FURNISHED TO DTIC
CONTAINED A SIGNIFICANT
NUMBER OF PAGES WHICH DO
NOT REPRODUCE LEGIBLY.

Crystal Structure, Reactivity, and Photochemical Properties of the Tungsten(0) Zwitterionic Amido Complex (CO)₅WNPhNPhC(OMe)Ph

Scott T. Massey, Nicholas D.R. Barnett, Khalil A. Abboud and Lisa McElwee-White*

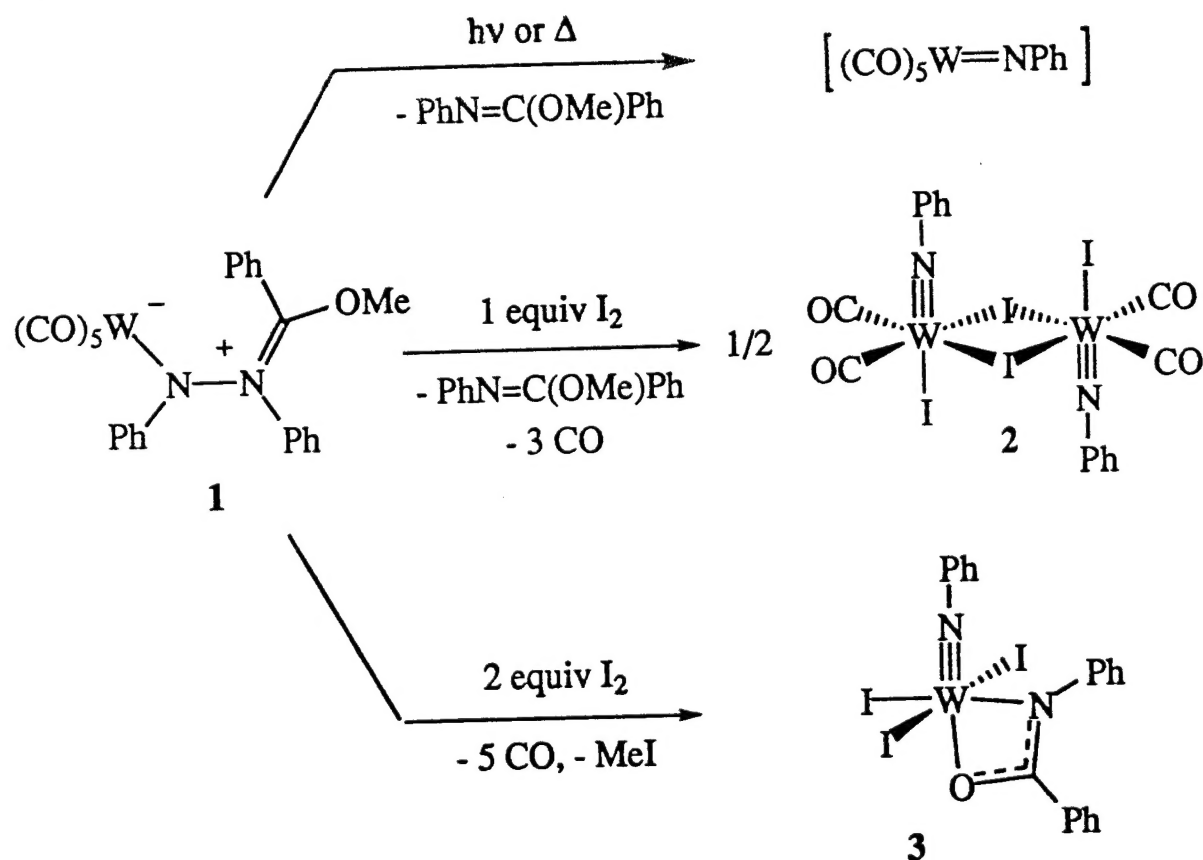Department of Chemistry, University of Florida, Gainesville, Florida 32611

Abstract

The crystal structure of the zwitterionic complex $(CO)_5WNPhNPhC(Ph)OMe$ (**1**) shows that it is best described as an amido complex in which the "imidate" fragment $PhN=C(Ph)OMe$ serves as a substituent on the amide nitrogen. The structural information allows the previously reported conversion of **1** to an isomeric zwitterion to be assigned as simple rotation about the N-C double bond. The twisted intermediate for such a rotation also offers a pathway for the previously reported isomerization of **1** to a 2,4-diazametallacycle. The electronic spectrum of **1** reveals a low energy MLCT transition that is responsible for its photodecomposition via N-N bond cleavage. INDO/1 CI calculations support assignment of the MLCT band as the HOMO to LUMO transition, where depopulation of the HOMO initiates the cleavage of the N-N bond.

Introduction

Amido complexes have proven to be valuable in the synthesis of transition metal imido compounds.[1] Although there are many useful synthetic methods that transfer the NR moiety from an organic substrate to the metal,[1,2] it is often more convenient to generate an imido ligand from a precursor in which the nitrogen is already bound to the metal. This has proven to be the case for low-valent metal imido complexes, which are particularly challenging targets because they are less stable than their higher-valent counterparts. The transformation of amides to imides has been used successfully by Brookhart and Templeton in the synthesis of low valent tungsten imido complexes.[3] These reactions typically involve hydride abstraction from the amide with Ph_3C^+ or deprotonation using a strong base.

1

Applying a somewhat different strategy, we have exploited the facile N-N bond cleavage of the zwitterionic amido complex $(CO)_5WNPhNPh(OMe)R$ [R = Me, Ph (1)] to generate the low valent imido compound $(CO)_5W=NPh$ as a reactive intermediate (Scheme 1).[4] Zwitterion 1 can also serve as a precursor to imido complexes in higher oxidation states. Chemical oxidation of 1 with 1 equiv of I_2 results in formation of W(IV) imido dimer 2 while reaction with 2 equiv of I_2 produces W(VI) metallacycle 3.[5] Both of these reactions have been demonstrated to occur through the same initial pathway, where oxidation of the W(0) center in 1 results in rapid N-N bond cleavage to give $PhN=C(OMe)Ph$ and reactive tungsten imido complexes.

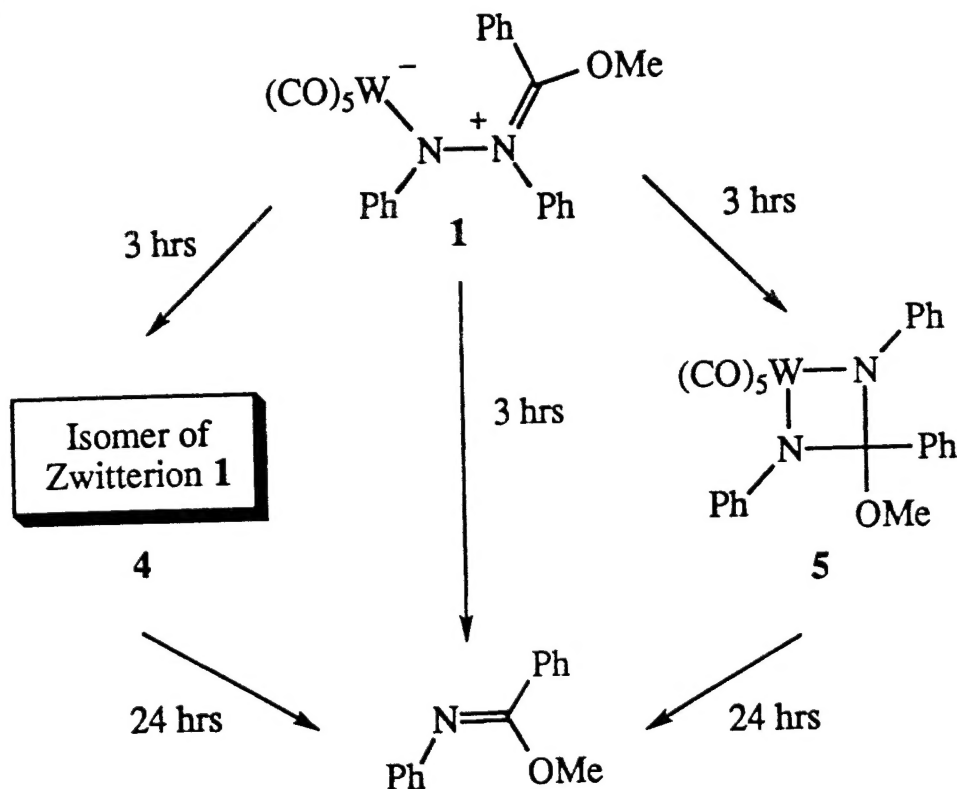**Scheme 1**

During our investigations on generation and trapping of $(CO)_5W=NPh$, extensive mechanistic studies on the decomposition of zwitterion 1 were carried out.[4a] Although no intermediates were detected under photolytic conditions, thermal decomposition of 1 at room

2

temperature revealed two intermediates which eventually decompose to give [(CO)$_5$W=NPh] and PhN=C(OMe)Ph (Scheme 2). Based on spectroscopic evidence, intermediate **4** was identified as an isomer of **1** although the site of isomerism that differentiates **1** from **4** could not be ascertained. Intermediate **5** was formulated as a 2,4-diazametallacycle.
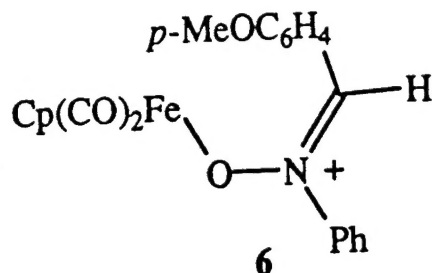
Scheme 2

We now report the X-ray crystal structure of **1**, which allows the stereochemistry of **4** to be assigned. Furthermore, the structure of **1** offers clues to its formation from (CO)$_5$W=C(OMe)Ph and *cis*-azobenzene and helps elucidate the mechanistic details for Scheme 2.[6] The electronic spectrum of zwitterion **1** is also examined and, with the aid of INDO/1 calculations, provides insight into the chemical and photochemical N-N bond scission observed for **1**.

Results and Discussion

Structure of Zwitterion 1. Although zwitterion **1** decomposes at room temperature in solution over the course of 3 hr, it is stable for weeks at -40 °C. Therefore, X-ray quality crystals of zwitterion **1** were grown from a cold chloroform solution which was slowly allowed to evaporate over a period of three weeks. This resulted in isolation of dark red needles that were washed in cold hexane and stored under an inert atmosphere. The crystal structure was obtained by coating a single crystal in Paratone® oil and placing it in a stream of cold N_2.

The crystal structure of **1** unequivocally confirms the atom connectivity originally derived from the spectroscopic data[4a,d] and in addition provides the conformation of **1**. A thermal ellipsoids diagram is shown in Figure 1 and selected structural data appear in Table 1. The geometry is octahedral at the metal, but with the CO ligands being distorted from perfect symmetry by the presence of the phenyl rings on N1 and N2. Evidence for the steric bulk of the amido ligand can be seen in the C1-W-N1 and C2-W-N1 angles of 98.4(2)° and 94.0(2)° respectively. Another effect of this steric crowding can be observed in the W-N1 bond length of 2.262(4) Å, which is considerably longer than the expected value of 1.952 Å for $W-NR_2$ bonds.[7] The W-N1 bond length is also longer than the W-N bond lengths of 2.125(5) and 2.156(5) Å in the W(0) bis(amido) complex $[Et_4N]_2[(CO)_3W(HNC_6H_4NH)]$.[8] The W-N1 bond lengthening in **1** also has an electronic origin that will be addressed later.

Another noteworthy feature is the N2-C13 bond length of 1.314(6) Å that lies in the range for C-N double bonds with a positive charge on the nitrogen.[9] The C=N bond of **1** is significantly longer than the C=N length of 1.270(8) Å observed in the related nitrone complex **6**,[10] however, indicating reduced double bond character with respect to **6**. Also of interest is the staggered helical arrangement of the three phenyl rings, which results in a chiral structure. The N2-C13 bond is perpendicular to the W-N1-N2 plane and the N2-C13 π system is thus unable to conjugate with the p orbital on N1. The p-orbital on N1 is instead conjugated into the phenyl ring, as evidenced by the short N1-C31 distance of 1.396(6) Å. All in all, **1** is best described as an amido complex in which the positively charged "imidate" fragment serves as a substituent on the amide nitrogen.
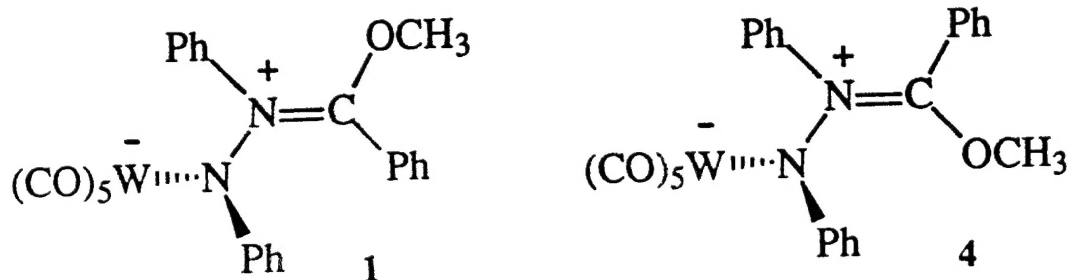
4

$$p\text{-MeOC}_6\text{H}_4$$

Cp(CO)$_2$Fe, structure with C=CH, O—N$^+$, Ph

6

The crystal structure of **1** confirms that the amido nitrogen possesses an almost perfectly planar geometry, as evidenced by the sum of 359.7° for the three bond angles about N1. Amido ligands are universally observed to adopt a planar geometry. This is a result of π-donation from the nitrogen lone-pair to a metal d orbital. Since the tetrahedral-to-planar distortion is relatively facile, even a small amount of donation from the nitrogen lone-pair will result in a planar amido ligand. In some systems, this $p_\pi \rightarrow d_\pi$ interaction is substantial enough to generate a measurable barrier to rotation about the M-NR$_2$ bond. However, the fact that the amido nitrogen in **1** is planar is not easily explained by simple electronic arguments, since there are no low-lying empty d-orbitals on the d^6 W(0) tungsten atom of **1** to accept p_π donation. Interaction between the nitrogen lone pair and filled d orbitals would be destabilizing, suggesting that the amido ligand should not bind well to the (CO)$_5$W fragment. This expectation is supported by the properties of the related W(0) bis(amido) complex [Et$_4$N]$_2$[(CO)$_3$W(HNC$_6$H$_4$NH)],[*] a molecule which accepts a five-coordinate, formally 16 e$^-$ configuration in order to accommodate π-donation from the amido ligands. Also of note with respect to the long W-N1 bond is the strong trans influence of the C5 carbonyl. The W-C5 bond length of 1.976(6) Å is significantly shorter than the average of 2.044 Å for the W-C distance of the other four carbonyls, each of which is trans to another.

MM2 calculations were performed to further probe the nature of this complex. The MM2 geometry optimization of **1**[11] resulted in a near-perfect planar arrangement of the amido nitrogen. Since these calculations contain no information on the electronic structure of the complex, this result suggests that steric congestion about the amido nitrogen forces the α-nitrogen into a planar structure. Therefore, steric considerations appear to override the electronic destabilization associated with planarity at N1.
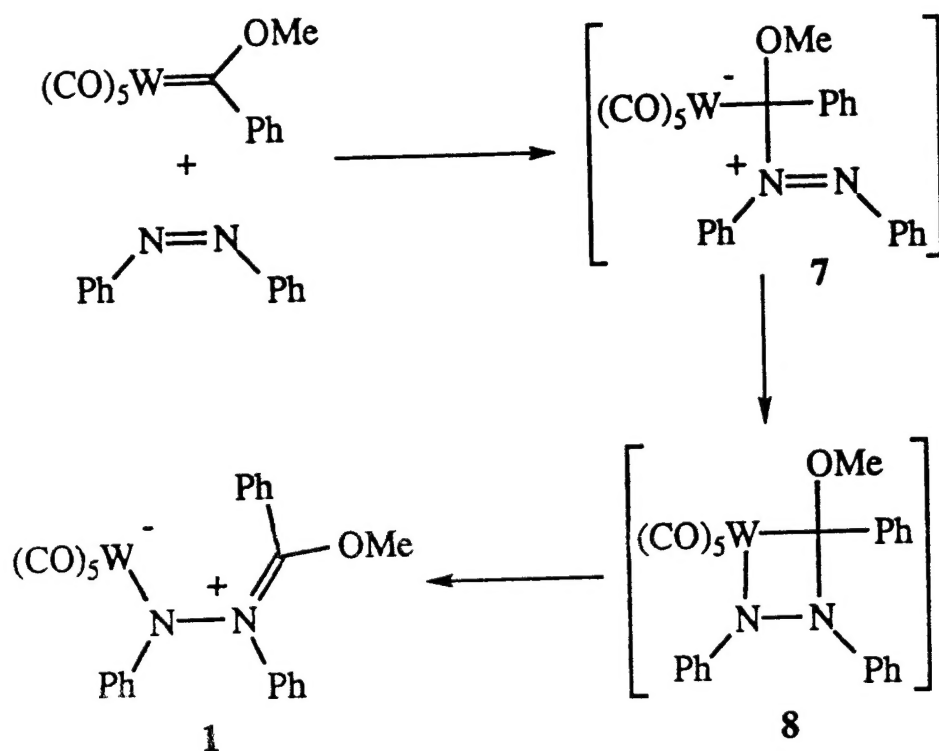
Formation of Zwitterion 1. Since the original spectroscopic data for $\mathbf{1}^{4a,b}$ established the connectivity of the zwitterion ligand but did not offer any clue to the three dimensional structure of the complex, the site of isomerism that differentiates **1** from **4** could not be ascertained. The crystal structure of **1**, however, allows a solution to this problem. Although crystallographic data on zwitterion **4** are not available, there exists only one reasonable site of isomerism: the C-N double bond. Since the phenyl groups of the "imidate" fragment are *trans* in **1**, they must then be *cis* in **4**. This leads to assignment of the isomeric zwitterion **4** as depicted.

In the reaction between $(CO)_5W=C(OMe)Ph$ and *cis*-azobenzene, zwitterion **1** is produced exclusively as the kinetic product and converts over time to the thermodynamically more stable isomer **4**. Therefore, any mechanism proposed for the reaction between the tungsten carbene and *cis*-azobenzene to give **1** must include an explanation of the preference for formation of the less stable *trans* isomer.
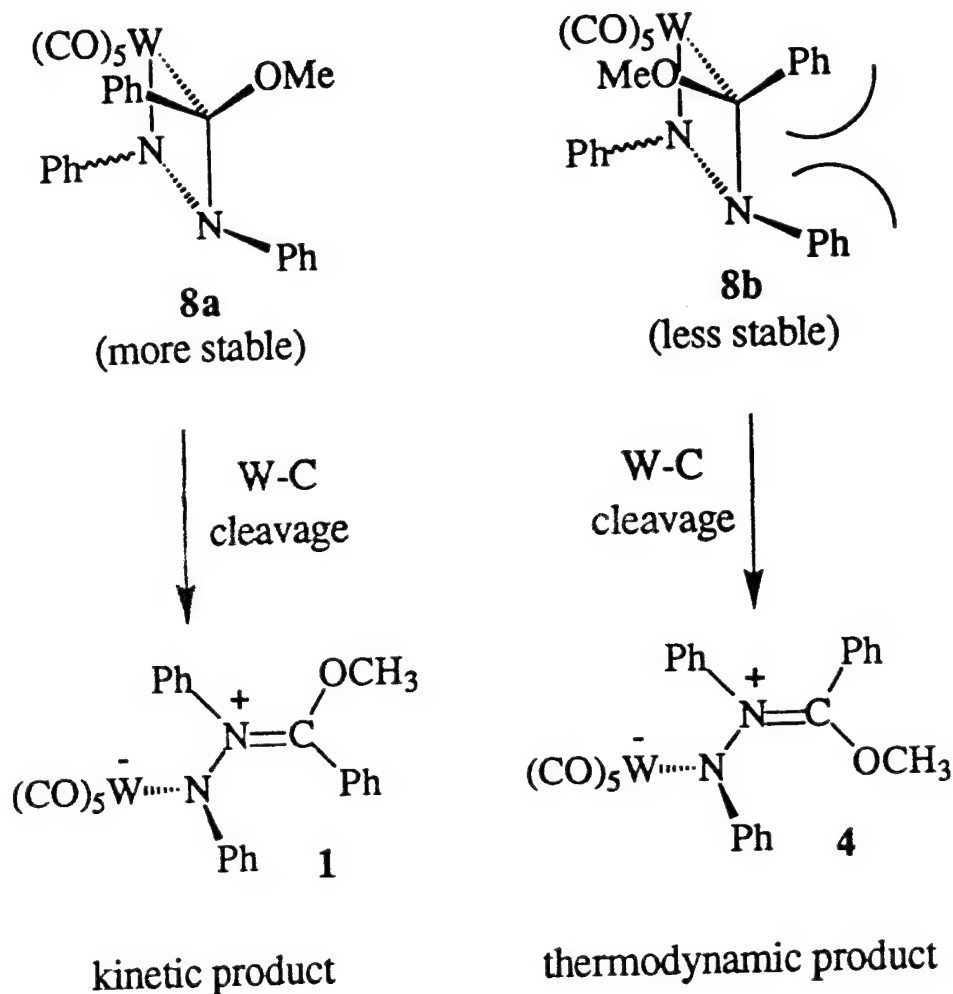
Given that *cis*-azobenzene reacts rapidly with $(CO)_5W=C(OMe)Ph$ while the *trans* azo compound is unreactive, the first step of this reaction is most likely the attack of the more nucleophilic nitrogen lone pair of *cis*-azobenzene on the electrophilic metal carbene carbon to form ylide **7** (Scheme 3). Although the ylide has not been observed in this reaction, a strong precedent exists for this intermediate since reactions between Fischer carbenes and Lewis bases such as tertiary phosphines and amines are known to give similar ylide complexes.[12]
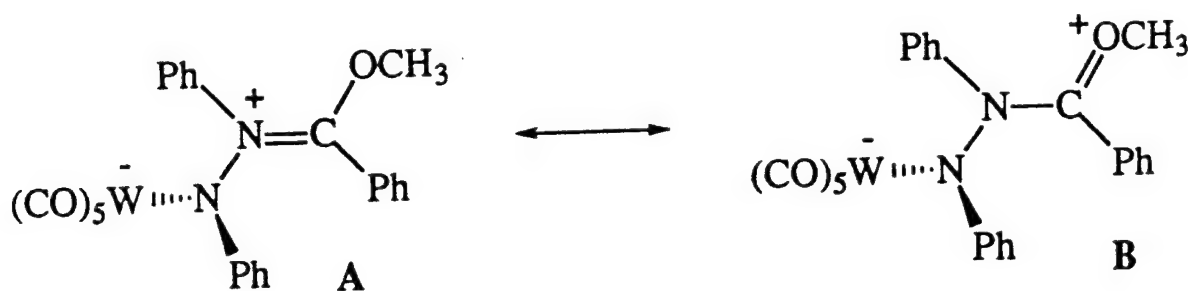
Scheme 3

Nitrogen-containing metallacycles have been proposed as intermediates or products in the reaction of a variety of unsaturated substrates with metal carbenes[10,13] and metal carbynes.[14] In fact, evidence for such a metallacycle in the related thermal reaction of $(CO)_5Cr=C(OMe)Me$ with cis-azobenzene has been reported.[6] Closure of ylide **7** to a four membered ring would result in metallacycle **8**, which upon W-C bond cleavage would yield a zwitterion.[15] Scheme 4 shows two possible stereochemistries at the ring C-N bond of **8**. Metallacycle **8b** would be less stable than **8a**, since there is an unfavorable steric interaction between the cis-phenyl groups. Molecular modeling (MM2)[11] estimates the energetic difference between **8a** and **8b** to be nearly 7 kcal/mol. To the extent that this developing steric interaction is present in the transition state for formation of **8b**, it would favor formation of **8a**, the precursor to the observed zwitterion **1**.

7

Scheme 4

8a
(more stable)

8b
(less stable)

W-C
cleavage

W-C
cleavage

1

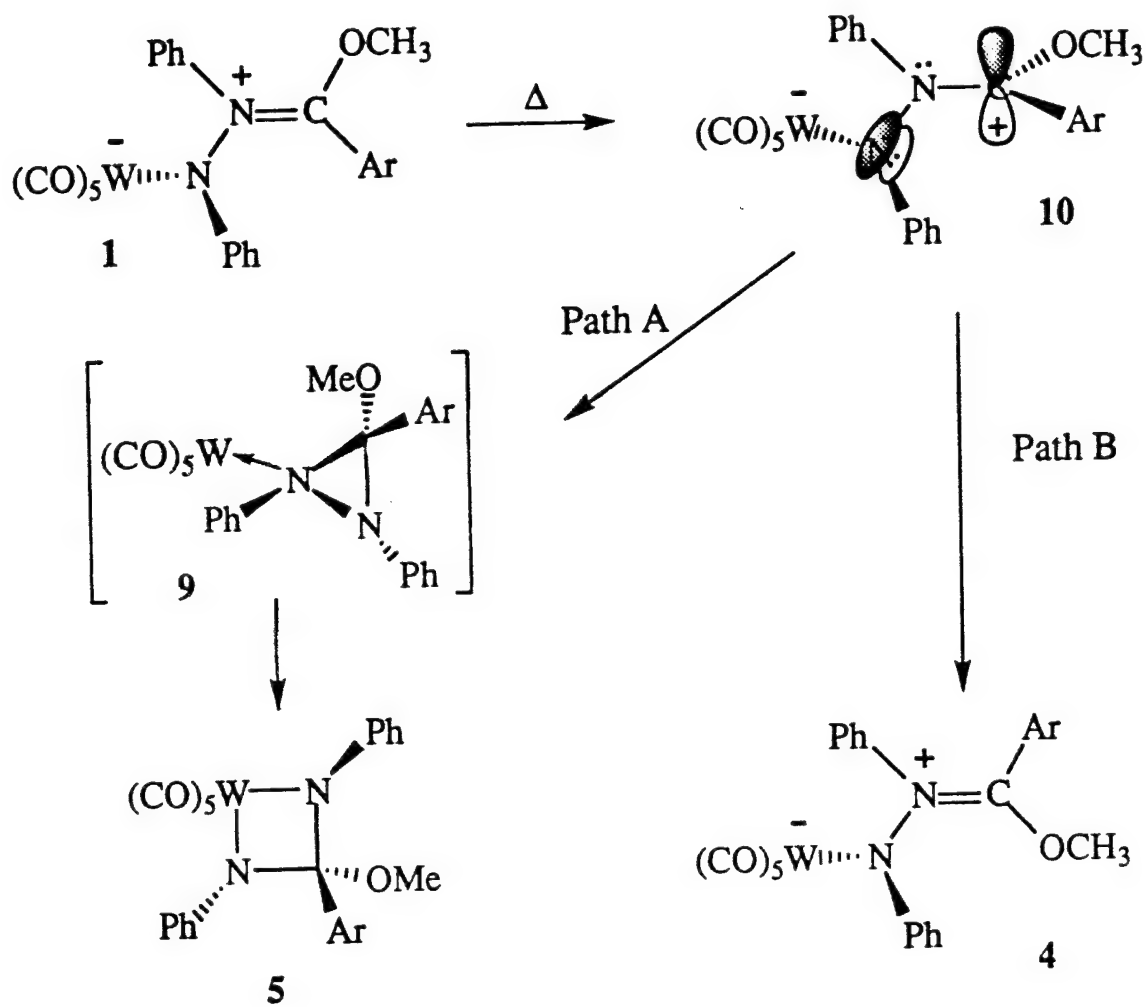kinetic product

4

thermodynamic product

Thermal Isomerization Reactions of Zwitterion 1. One mechanism that would account for the isomerization of **1** to **4** involves a simple rotation about the N-C double bond. Although the barrier to isomerization about the double bond of a neutral imidate through either rotation about the bond or inversion at the nitrogen is known to be large,[16] a positively charged nitrogen should lower this barrier by increasing the involvement of the oxygen lone-pair. In fact, under conditions where an imidate is protonated the rate of isomerization has been observed to increase.[17] The participation of resonance structure **B** coupled with the sterically demanding environment in **1** are consistent with the relatively facile conversion of zwitterion **1** to **4**.
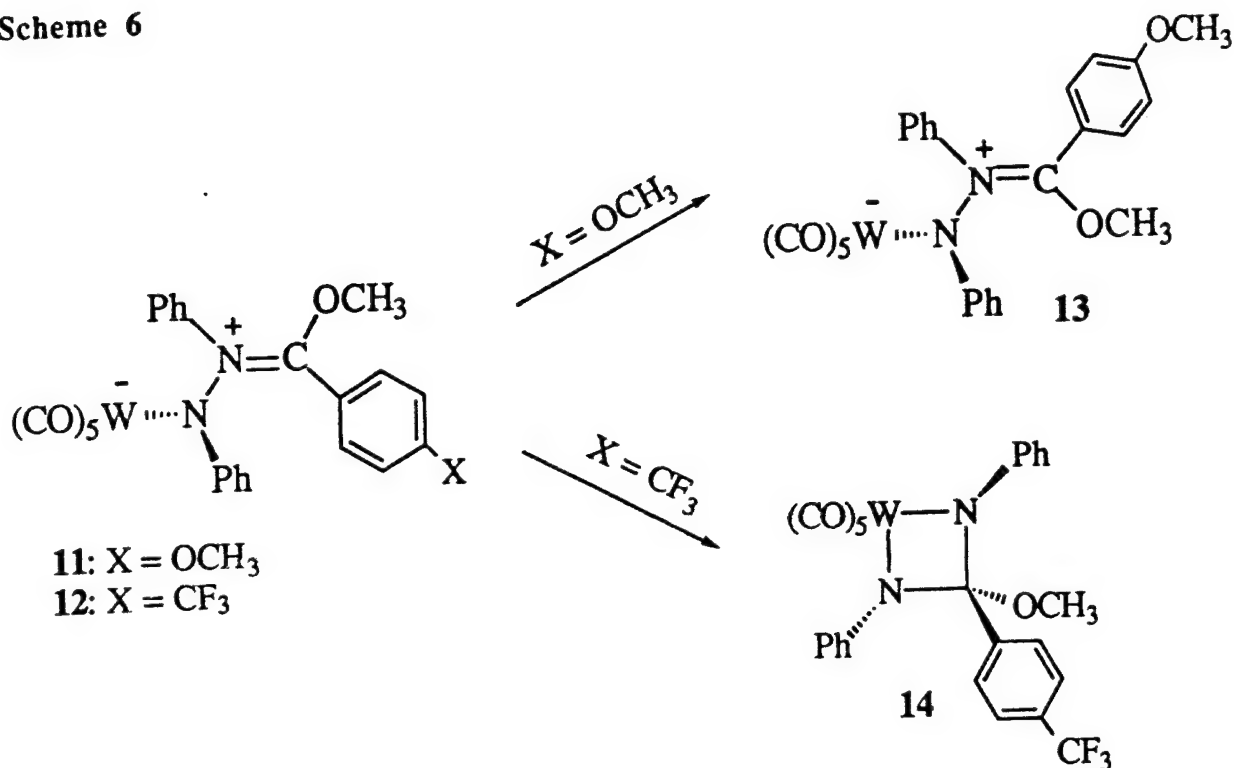
If rotation about the N-C double bond is the operative mechanism that converts **1** to **4**, the intermediate in this isomerization pathway may also be shared by the pathway which converts zwitterion **1** to the 2,4-diazametallacycle **5** (Scheme 5). Diaziridine complex **9** has previously been demonstrated to be an intermediate in the conversion of **1** to **5**.[4a] As shown in Scheme 5, the twisted intermediate **10** is a reasonable common element between path A to diaziridine complex **9** and path B to the isomerized zwitterion **4**. Path B results when species **4** completes rotation about the N-C bond, whereas path A results from the attack of the amido nitrogen on the empty carbon p orbital.

Additional experiments which support the involvement of **10** as the focal point between path A and path B (Scheme 5) are shown in Scheme 6. The thermal decompositions of zwitterions **11** and **12**[4a] result in very different product distributions. In the case of the more electron rich **11**, the major product is the isomeric zwitterion **13**. The *p*-methoxy substituent is capable of stabilizing the positive charge that develops at the benzylic carbon in **10** by resonance, thus slowing attack of the amide lone pair on the benzylic carbon. Completion of the C-N rotation to yield **4** then dominates reactivity (path B in Scheme 5). For zwitterion **12**, the primary product is the 2,4-diazametallacycle **14**. Since the *p*-CF$_3$ group on **12** destabilizes the developing positive charge at the benzylic position of **10**, the intermediate is much more susceptible to intramolecular attack by the amide nitrogen (path A in Scheme 5).

9

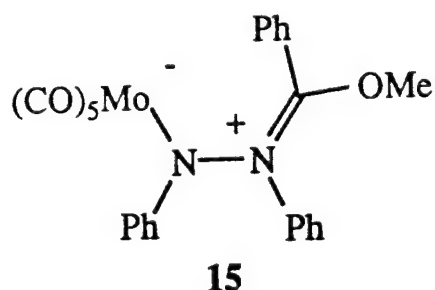**Scheme 5**

Scheme 6

11: X = OCH$_3$
12: X = CF$_3$

Photochemistry of Zwitterion 1. Zwitterion **1** is a black powder that readily dissolves in polar solvents to give dark-colored solutions. The observation that very dilute solutions of zwitterion **1** appear green in toluene and red in methylene chloride prompted the study of its UV-visible spectrum. The spectrum of **1** in methylene chloride (Figure 2a) shows strong absorbances at short wavelengths, which tail into the visible region of the spectrum. The band primarily responsible for the observed color of **1**, however, is a relatively weak band found at 556 nm which appears as a shoulder on the higher energy transitions. The zwitterionic nature of **1**, with its negative charge on the metal and positively charged nitrogen suggested the possibility that the shoulder band is a metal-to-ligand-charge-transfer (MLCT) transition.[18]

In an MLCT transition, the solvation of the ground state may differ significantly from that of the excited state, leading to solvatochromism.[19] When the ground state is more effectively solvated by polar solvents than the excited state, negative solvatochromism is the result (i.e. the MLCT band blue-shifts upon increasing solvent polarity). This situation would be expected for

MLCT states of zwitterion **1**, where the ground state charge separation would be decreased upon charge transfer to the ligand. The assignment of the absorption at 556 nm as a low energy MLCT band was confirmed by observing the solvent dependence of its λ_{max}. Shown in Figure 2b is a series of UV-vis spectra of zwitterion **1** taken in four different solvents ranging in polarity from toluene to acetonitrile. Increasing the polarity of the solvent causes a significant blue-shift in the maximum absorption of the MLCT band, while the rest of the UV-vis spectrum appears unchanged.

Calculations using the INDO model Hamiltonian in the program ZINDO[20] have proven valuable in examining the electronic transitions of zwitterion **1**. The calculations were performed on the molybdenum zwitterion **15** as a model compound for its tungsten congener **1**. The atomic coordinates for **15** were taken directly from the crystal structure of **1** and the calculation was done using INDO/1 parameters. The HOMO and LUMO of the model zwitterion **15** are depicted in Figure 3. The HOMO is primarily a metal-nitrogen π^* molecular orbital and the LUMO is a π^* MO centered on the "imidate" fragment of the zwitterion ligand.

15

An electronic spectrum was generated from configuration interaction (CI) calculations on **15** (Figure 4). Although the relative absorbances and maxima do not match the spectrum of **1** precisely, the general features of the calculated spectrum closely resemble those of Figure 2a. Of significance in the calculated spectrum is the low energy HOMO to LUMO transition at 540 nm which corresponds to the MLCT band in the observed spectrum. Calculations using different simulated solvent environments reproduced the blue shifts of the low energy transition of **1** in more polar solvents, consistent with assignment of the MLCT band as the HOMO to LUMO transition.

Upon low temperature photolysis using a medium-pressure mercury vapor lamp, zwitterion 1 decomposes to give imidate PhN=C(OMe)Ph in high yield as the only identifiable product. Trapping experiments have demonstrated that the other primary photoproduct is the unstable nitrene complex (CO)$_5$W=NPh.[4b,c] Although zwitterion 1 is perfectly stable in solution at low temperatures, photolysis of 1 in toluene at -50 °C using a Corning-555 long pass filter to block wavelengths shorter than 555 nm results in disappearance of the starting material after 3 hr. The photodecomposition rate of 1 in toluene is comparable to the rate of photolysis in a control sample using unfiltered radiation under the same conditions. In addition, gas chromatography (GC) demonstrated that the same amount of imidate PhN=C(OMe)Ph was produced in comparison to the control sample. This experiment illustrates that excitation to the MLCT state is responsible for photochemical decomposition of 1 via N-N bond cleavage.
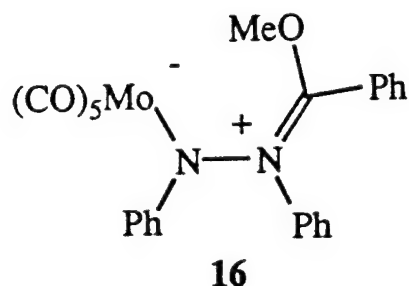
The INDO/1 study of zwitterion 15 discussed above suggests that removing an electron from the HOMO of 1, a W-N π^* orbital, will strengthen the W-N bond in the excited state. Although a weakening of the N-N bond is not an obvious consequence of this excitation, the increased bonding interactions between the tungsten and amido nitrogen in the MLCT excited state may cause structural changes which favor N-N bond cleavage to give PhN=C(OMe)Ph and (CO)$_5$W=NPh. The MLCT transition seen in zwitterion 1 is not typical, in that excitation results in a photochemical reaction. In most MLCT excitations of organometallics, the transition originates in a metal centered non-bonding d orbital and terminates in a ligand-localized orbital that does not influence metal-ligand bonding.[1a,21] The excited state then undergoes electron transfer, luminescence or non-radiative decay. The MLCT transition in 1 is different in that it originates from a metal-ligand antibonding orbital. The bonding between the metal and ligand is thus significantly altered upon excitation and a chemical reaction follows.

Photochemistry of Zwitterion 4. Over the course of 3 hr, a solution of 1 in CH$_2$Cl$_2$ turns from black to red. Zwitterion 4 can be isolated as a brown powder in low yield by the addition of cold hexane to this solution. This zwitterion, however, appears red in solution and its color is independent of the nature of the solvent. The UV-vis spectrum of 4 shows some of the

13

same features as the spectrum of **1**, although it is not as well resolved. Surprisingly, the MLCT band could not be found. Even at much higher concentrations in a number of different solvents, the UV-vis spectrum did not reveal a transition analogous to the MLCT band in the spectrum of **1**.

As was done for zwitterion **1**, INDO/1 calculations were performed on the molybdenum zwitterion **16** as a model compound for its tungsten congener **4**. The coordinates of the atoms in the $(CO)_5MoN$ fragment of **16** were obtained from the X-ray structure of **1**. The rest of the geometry was obtained by MM2 optimization with the $(CO)_5MoN$ fragment locked in place. An electronic spectrum was generated from configuration interaction (CI) calculations on **16**. The MLCT band is clearly present in the simulated spectrum but is strongly red shifted to 796 nm. Since the calculated position of the band is near the long wavelength limit of the spectrometer, it is possible that it was not detected because it lies too far to the red. However, the existence of the MLCT transition may be inferred from the observation that photolysis of **4** leads to N-N bond cleavage to give the imidate PhN=C(OMe)Ph, a photochemical process that was attributed to the MLCT excited state in **1**.

$$
\begin{array}{c}
\text{MeO} \\
(CO)_5Mo\diagdown \quad \overset{-}{} \quad \diagup\text{Ph} \\
\diagdown \quad \overset{+}{} \diagup \\
N\!\!-\!\!N \\
\diagup \quad \diagdown \\
\text{Ph} \qquad \text{Ph}
\end{array}
$$

16

Oxidation of Zwitterion 1. As discussed above, the low energy transition that initiates N-N bond cleavage of **1** was assigned as the HOMO to LUMO excitation where the HOMO is an antibonding orbital between the tungsten and the amido nitrogen. Depopulation of the HOMO is expected to strengthen the W-N bond, providing the impetus for N-N bond cleavage. Since photoexcitation of **1** at the MLCT band results in a formal oxidation of the metal center (and N-N cleavage), the possibility that electrochemical oxidation would also result in N-N bond cleavage was considered. In the cyclic voltammogram of **1**, a single irreversible oxidation is observed at 1.27 V (vs. SHE) at -78 °C in CH_2Cl_2/TBAH. Scans taken at up to 1 V/s showed no sign of

14

reversibility. In addition, scanning the potential region positive of the oxidation wave gave no indication of another oxidizable material within the solvent window. A cyclic voltammogram of PhN=C(OMe)Ph in CH_2Cl_2/TBAH at 25°C showed an irreversible oxidation at 1.69 V. While oxidation of **1** would be expected to yield imidate, no evidence for this compound was observed. Since scanning to higher potentials after the oxidation wave of **1** resulted in an irreversible $Cp_2Fe(III)/Cp_2Fe(II)$ wave on the reverse scan, we can conclude that attempts to observe imidate were thwarted by electrode plating during the forward scan.

Although the electrochemical study did not provide much insight into the oxidation of zwitterion **1**, the E_p of 1.27 V (vs. SHE) suggests that a wide range of oxidants will react with **1**. This conclusion was borne out in the reaction of zwitterion **1** with I_2, where W(IV) and W(VI) imido complexes are generated along with the imidate PhN=C(OMe)Ph or MeI as a side-product.[5]

Conclusion. The crystal structure of zwitterion **1** (Figure 1) has allowed the assignment of the stereochemistry for **1** and its isomer **4**. The exclusive formation of **1** in the reaction of *cis*-azobenzene with $(CO)_5W=C(OMe)Ph$ can be explained in terms of the relative stability of the intermediate metallacycles **8a** and **8b**. The isomerization of **1** to **4** is proposed to be a simple rotation about the N=C bond. The twisted intermediate in this isomerization (**10**) also offers a direct route to the coordinated diaziridine intermediate **9**, the precursor to 2,4-diazametallacycle **5**. The proposed mechanism (Scheme 5) is supported by experiments in which *para*-substitution of the phenyl ring significantly alters the product distribution of zwitterion **4** and 2,4-diazametallacycle **3**, consistent with positive charge developing at the benzylic position in the intermediate.

The crystal structure of zwitterion **1** confirms that the amido nitrogen is planar. Electronic arguments do not adequately explain the planar geometry about the amide nitrogen, but MM2 calculations suggest that the amido nitrogen is planar due to steric interactions between the phenyl rings on the "imidate" fragment and the tungsten carbonyls. This planar geometry has a direct effect on the electronic spectrum of **1**, where a low energy MLCT band was found to be the HOMO to LUMO transition. The HOMO is a π^* antibonding orbital between the metal and amido

15

nitrogen. Depopulation of this orbital by photooxidation (or chemical oxidation) of the metal center in **1** strengthens the W-N bond, initiating N-N bond cleavage and the formation of PhN=C(OMe)Ph. Photolytic N-N bond cleavage in **1** at long wavelengths (above 555 nm) in toluene supports this hypothesis.

Experimental Section.

General. Standard inert atmosphere Schlenk, cannula, and glove box techniques and freshly distilled solvents were used in all experiments unless stated otherwise. THF was distilled from Na/Ph$_2$CO. Toluene was distilled over sodium. CH$_2$Cl$_2$ was distilled over CaH$_2$. CH$_3$CN was degassed by three freeze-pump-thaw cycles and stored over 3 Å molecular sieves under N$_2$. All chemicals were purchased in reagent grade and used with no further purification unless stated otherwise. Zwitterions **1** and **4** were prepared according to previously published methods.[4a,5b] PhN=C(OMe)Ph was synthesized according to the method reported by Lander.[22] Electrochemical experiments were performed under nitrogen using an IBM EC225 Voltammetric Analyzer. Cyclic voltammograms were recorded in a standard three-electrode cell with a glassy carbon working electrode. All potentials are reported vs. NHE and were determined in CH$_2$Cl$_2$. Ferrocene ($E_{1/2}$ = 0.55 V) was used *in situ* as a calibration standard. Analytical GC was performed on a HP5890A chromatograph containing a 5 m x 0.25 mm column of SE-54 on fused silica. UV-vis spectra were recorded using a Hewlett-Packard 8450A diode array spectrophotometer. All photolysis experiments were performed in 5 mm NMR tubes or Schlenk tubes by irradiation with a Hanovia medium pressure mercury vapor lamp in a Pyrex immersion well. Computational chemistry was performed on a Macintosh Quadra 950 using a CAChe system.[11]

Crystal Structure of 1. Data were collected at 173 K on a Siemens SMART PLATFORM equipped with a CCD area detector and a graphite monochromator utilizing MoK$_\alpha$ radiation (λ = 0.71073 Å). Cell parameters were refined using the entire data set. A hemisphere of data (1321 frames) was collected using the ω-scan method (0.3° frame width). The first 50 frames were remeasured at the end of data collection to monitor instrument and crystal stability

(maximum correction on I was < 1 %). Psi scan absorption corrections were applied based on the entire data set.

The structure was solved by the Direct Methods in *SHELXTL5*,[23] and refined using full-matrix least squares. The non-H atoms were treated anisotropically, whereas the hydrogen atoms were calculated in ideal positions and were riding on their respective carbon atoms. 308 parameters were refined in the final cycle of refinement using 4779 reflections with $I > 2\sigma(I)$ to yield R_1 and wR_2 of 3.34 and 7.66 , respectively. Refinement was done using F^2.

Cyclic Voltammetry of Zwitterions 1 and 4. The following procedure was followed for both zwitterions **1** and **4**. Ferrocene (20 mg, 0.11 mmol) and anhydrous $Bu_4N^+PF_6^-$ (450 mg, 1.16 mmol) were dissolved in dry CH_2Cl_2 (20 mL). The solution was added to an electrochemical cell under an N_2 purge and cooled to -78 °C in a dry ice/acetone bath. Zwitterion (40 mg, 0.063 mmol) was then added, and the solution was kept under an N_2 purge before and after measurements were taken. Cyclic voltammetry measurements were typically run at 100 mV/s using ferrocene as a reference (0.55 V vs. NHE). CV: **1**: E_p = 1.27 V; **4**: E_p = 1.30 V.

UV-vis Spectroscopy of Zwitterions 1 and 4. The following procedure is typical. Solutions were prepared in an inert atmosphere box. All glassware, solvents, and cuvettes were cooled to -40 °C before the solutions were prepared and the UV-vis measurements obtained. Spectroscopic data were collected at low concentrations of **1** in toluene (1.285×10^{-4} M), CH_2Cl_2 (2.640×10^{-5} M), THF (2.652×10^{-5} M), and CH_3CN (2.684×10^{-5} M) over a 200 - 800 nm range. Spectra were obtained at higher concentrations of **1** in toluene (1.294×10^{-3} M), CH_2Cl_2 (1.390×10^{-3} M), THF (1.326×10^{-3} M), and CH_3CN (1.342×10^{-3} M) for observation of the solvent dependence of the MLCT band. These data were collected over a 450 - 750 nm range. The UV-vis spectrum of **1** is shown in Figure 2.

Photolysis of Zwitterion 1 at Wavelengths Greater Than 555 nm. Zwitterion **1** (25.6 mg, 0.0409 mmol) was dissolved in 5 mL of cold toluene (-40 °C). 1 mL aliquots of the solution were added to two NMR tubes. One sample was placed behind a corion LG-555 filter and submerged in an acetonitrile/dry ice bath. Both samples were photolyzed at -50 °C. Photolysis of

the samples was judged complete when the dark green color of the solutions had completely disappeared. Photolysis of the control sample (unfiltered radiation) was complete within 2.5 hr, whereas the sample photolyzed behind a filter required 3 hr. GC analysis indicated that a similar yield of PhN=C(OMe)Ph had been produced in each sample. Another reaction was performed to determine the yield of imidate produced using a long-pass filter. Zwitterion **1** (19.8 mg, 0.0316 mmol) was placed in a cooled Schlenk tube and 15 mL of precooled toluene (-40 °C) was added. The tube was fitted with a corion LG-555 filter and photolyzed for 8 hr at -50 °C. The solution was concentrated under vacuum, then diluted to 1 mL. A GC analysis using a standard solution of imidate PhN=C(OMe)Ph showed that photodecomposition of zwitterion **1** at wavelengths above 555 nm resulted in a 64% yield of imidate PhN=C(OMe)Ph.

Supporting Information Available. Tables of crystallographic data, bond distances, bond angles, positional parameters, and anisotropic displacement parameters for **1** (7 pages). This material is contained in many libraries on microfiche, immediately follows this article in the microfilm version of the journal, and can be ordered from the ACS, and can be downloaded from the Internet; see any current masthead page for ordering information and Internet access instructions.

References

1. Wigley, D.E. *Prog. Inorg. Chem.*, **1994**, *42*, 239-482.

2. a) Nugent, W.A.; Haymore, B.L. *Coord. Chem. Rev.*, **1980**, *31*, 123-175. b) Cenini, S.; La Monica, G. *Inorg. Chim. Acta*, **1976**, *18*, 279-293.

3. a) Pérez, P. J.; White, P. S.; Brookhart, M.; Templeton, J. L. *Inorg. Chem.*, **1994**, *33*, 6050-6056. b) Powell, K. R.; Pérez, P. J.; Luan, L.; Feng, S. G.; White, P. S.; Brookhart, M.; Templeton, J. L. *Organometallics*, **1994**, *13*, 1851-1864. c) Pérez, P. J.; Luan, L.; White, P. S.; Brookhart, M.; Templeton, J. L. *J. Am. Chem. Soc.*, **1992**, *114*, 7928-7929. d) Luan, L.; White, P. S.; Brookhart, M.; Templeton, J. L. *J. Am. Chem. Soc.*, **1990**, *112*, 8190-8192.

4. a) Maxey, C. T.; Sleiman, H. F.; Massey, S. T.; McElwee-White, L. *J. Am. Chem. Soc.*, **1992**, *114*, 5153-5160. b) Arndtsen, B. A.; Sleiman, H. F.; Chang, A. K.; McElwee-White, L. *J. Am. Chem. Soc.*, **1991**, *113*, 4871-4876. c) Sleiman, H. F.; Mercer, S.; McElwee-White, L. *J. Am. Chem. Soc.*, **1989**, *111*, 8007-8009. d) Sleiman, H. F.; McElwee-White, L. *J. Am. Chem. Soc.*, **1988**, *110*, 8700-8701.

5. a) McGowan, P. C.; Massey, S. T.; Abboud, K. A.; McElwee-White, L. *J. Am. Chem. Soc.*, **1994**, *116*, 7419-7420. b) Barnett, N.D.R.; Massey, S.T.; McGowan, P.C.; Wild, J.J.; Abboud, K.A.; McElwee-White, L. *Organometallics*, **1996**, *15*, 424-428.

6. Related chemistry with chromium complexes has been reported by Hegedus. a) Hegedus, L.S.; Kramer, A. *Organometallics*, **1984**, *3*, 1263-1267. b) Hegedus, L.S.; Lundmark, B.R. *J. Am. Chem. Soc.*, **1989**, *111*, 9194-9198.

7. Orpen, A.G.; Brammer, L.; Allen, F.H.; Kennard, O.; Watson, D.G.; Taylor, R. *J. Chem. Soc., Dalton Trans.*, **1989**, S1-S83.

8. Darensbourg, D.J.; Klausmeyer, K.K.; Reibenspies, J.H. *Inorg. Chem.*, **1996**, *35*, 1535-1539.

9. Allen, F.H.; Kennard, O.; Watson, D.G.; Brammer, L.; Orpen, A.G.; Taylor, R. *J. Chem. Soc., Perkin Trans. 2*, **1987**, S1-S19.

10. Peng, W.-J.; Gamble, A.S.; Templeton, J.L.; Brookhart, M. *Inorg. Chem.*, **1990**, *29*, 463-467.

11. CAChe WorkSystem, Release 3.8. CAChe Scientific, Beaverton, Oregon.

12. a) Kreissl, F.R.; Fischer, E.O.; Kreiter, C.G.; Fischer, H. *Chem. Ber.*, **1973**, *106*, 1262-1276. b) Fischer, H.; Fischer, E.O.; Kreiter, C.G.; Werner, H. *Chem. Ber.*, **1974**, *107*, 2459-2467. c) Fischer, H. *J. Organomet. Chem.*, **1979**, *170*, 309-317. d) Kreissl, F.R.; Fischer, E.O.; Kreiter, C.G.; Weiss, K. *Angew. Chem. Int. Ed. Eng.*, **1973**, *12*, 563. e) Kreissl, F. R.; Fischer, E.O. *Chem. Ber.*, **1974**, *107*, 183-188.

13. a) Fischer, H.; Zeuner, S. *J. Organomet. Chem.*, **1987**, *327*, 63-75. b) Fischer, H.; Märkl, R. *Chem. Ber.*, **1985**, *118*, 3683-3699. c) Maxey, C.T.; McElwee-White, L. *Organometallics*, **1991**, *10*, 1913-1916. d) Pilato, R.S.; Williams, G.D.; Geoffroy, G.L.; Rheingold, A.L. *Inorg. Chem.*, **1990**, *29*, 463-467.

14. a) Mercando, L.A.; Handwerker, B.M.; MacMillan, H.J.; Geoffroy, G.L.; Rheingold, A.L.; Owens-Waltermire, B.E. *Organometallics*, **1993**, *12*, 1559-1574. b) Handwerker, B.M.; Garrett, K.E.; Nagle, K.L.; Geoffroy, G.L.; Rheingold, A.L. *Organometallics*, **1990**, *9*, 1562-1575. c) Handwerker, B.M.; Garrett, K.E.; Geoffroy, G.L.; Rheingold, A.L. *J. Am. Chem. Soc.*, **1989**, *111*, 369-371.

15. It is also possible to devise mechanisms for the conversion of **7** to **1** that involve migration of tungsten instead of the intermediacy of **8**. However, isolation of the isomeric metallacycle **5** from this system lends credence to the transient existence of **8**.

16. Foder, G. and Phillips, B.A. in *Chemistry of Amidines and Imidates*, John Wiley & Sons, **1975**.

17. Moriarty, R.M.; Yeh, C-L; Kermit, C.R.; Whitehurst, P.W. *J. Am. Chem. Soc.*, **1970**, *92*, 6360-6362.

18. a) Meyer, T.J. *Pure Appl. Chem.*, **1986**, *58*, 1193-1206. b) Roundhill, D.M. *Photochemistry and Photophysics of Metal Complexes*; Plenum Press: New York, **1994**.

19. a) Kaim, W.; Kohlmann, S.; Ernst, S.; Olbrich-Deussner, B.; Bessenbacher, C.; Schulz, A. *J. Organomet. Chem.*, **1987**, *321*, 215-226. b) Manuta, D.M.; Lees, A.J. *Inorg. Chem.*, **1983**, *22*, 3825-3830.

20. Zerner, M.C., *et al.*, Department of Chemistry, University of Florida.

21. Geoffroy, G.L.; Wrighton, M.S. *Organometallic Photochemistry*; Academic Press: New York, **1979** pp. 15-18.

22. Lander, G. D. *J. Chem. Soc.*, **1902**, 591-598.

23. Sheldrick, G. M. *SHELXTL5*. Nicolet XRD Corporation, Madison, Wisconsin, USA.

Table 1. Selected bond lengths [Å] and angles [°] for **1.**

W-C(5)	1.976(6)
W-C(2)	2.019(5)
W-C(1)	2.047(6)
W-C(3)	2.054(6)
W-C(4)	2.055(6)
W-N(1)	2.262(4)
N(1)-C(31)	1.396(6)
N(1)-N(2)	1.422(6)
N(2)-C(13)	1.314(6)
N(2)-C(41)	1.455(6)
C(5)-W-N(1)	174.2(2)
C(31)-N(1)-N(2)	112.2(4)
C(31)-N(1)-W	130.1(3)
N(2)-N(1)-W	117.4(3)
C(13)-N(2)-N(1)	120.0(4)
N(2)-C(13)-C(21)	123.2(4)
O(6)-C(13)-C(21)	121.7(4)
W-N(1)-N(2)-C(13)	-123.8(4)

Table 2. Crystal data and structure refinement for **1**.

empirical formula	$C_{25}H_{18}N_2O_6W$
formula weight	626.26
temperature	173(2) K
wavelength	0.71073 A
crystal system	triclinic
space group	P $\bar{1}$
unit cell dimensions	a = 8.3071(2) Å $\quad$ α = 76.459(1) °
	b = 11.4298(2) Å $\quad$ β = 86.425(1) °
	c = 12.9757(2) Å $\quad$ γ = 79.896(1) °
volume, Z	1178.91(4) Å^3
density (calculated)	1.764 Mg/m^3
absorption coefficient	4.942 mm^{-1}
F(000)	608
crystal size	0.23 x 0.14 x 0.07 mm
θ range	1.61 - 27.50 °
limiting indices	$-9 \leq h \leq 10, -12 \leq k \leq 14, -16 \leq l \leq 15$
reflections collected	6918
independent reflections	4819 [R(int) = 0.0359]
refinement method	full-matrix least-squares on F^2
data / restraints / parameters	4779 / 0 / 308
goodness-of-fit on F^2	1.056
final R indices [I > 2σ(I)]	R1 = 0.0334, wR2 = 0.0766
R indices (all data)	R1 = 0.0387, wR2 = 0.0829
extinction coefficient	0.0000(3)
largest diff. peak and hole	2.690 and -1.002 e Å^{-3}

Figure Captions

Figure 1. Thermal ellipsoids diagrams of **1** showing the crystallographic numbering scheme. Ellipsoids are drawn at the 40% probability level.

Figure 2. (a) UV-vis spectrum of **1** in CH_2Cl_2 with the weak low energy transition shown as an inset. (b) Solvent dependence of MLCT transition in **1** [λ_{max} in nm, (ϵ)]: toluene: 580 (1360); CH_2Cl_2: 556 (1330); THF: 552 (1190); CH_3CN: 526 (1120).

Figure 3. Frontier orbitals of **1**. Orbital surfaces are taken from ZINDO calculations as described in text and plotted with an isosurface value of 0.07. (a) HOMO. (b) LUMO.

Figure 4. Calculated UV-vis spectrum of **15** in the absence of solvent. Absorptions and extinction coefficients are taken from ZINDO-CI calculations as described in text.
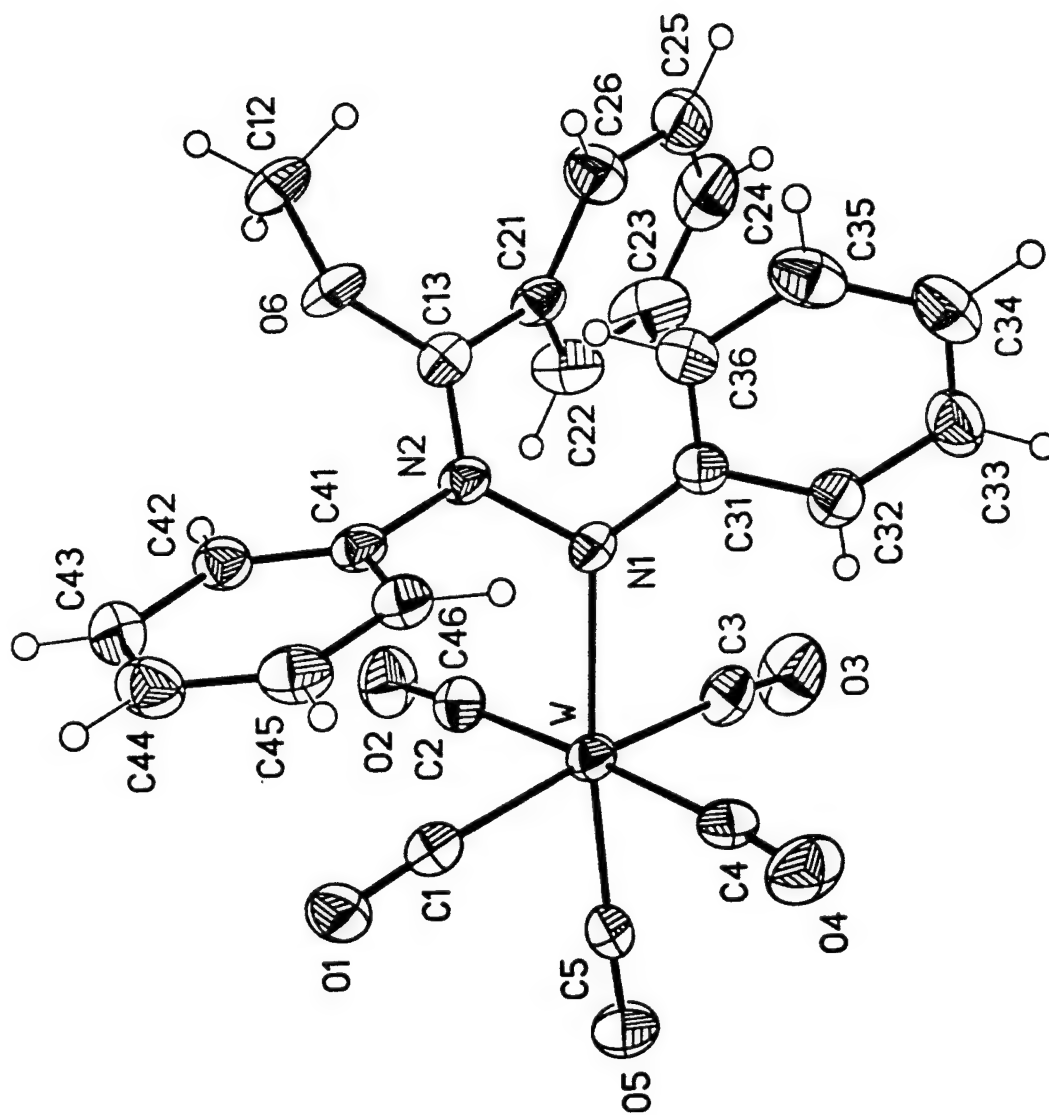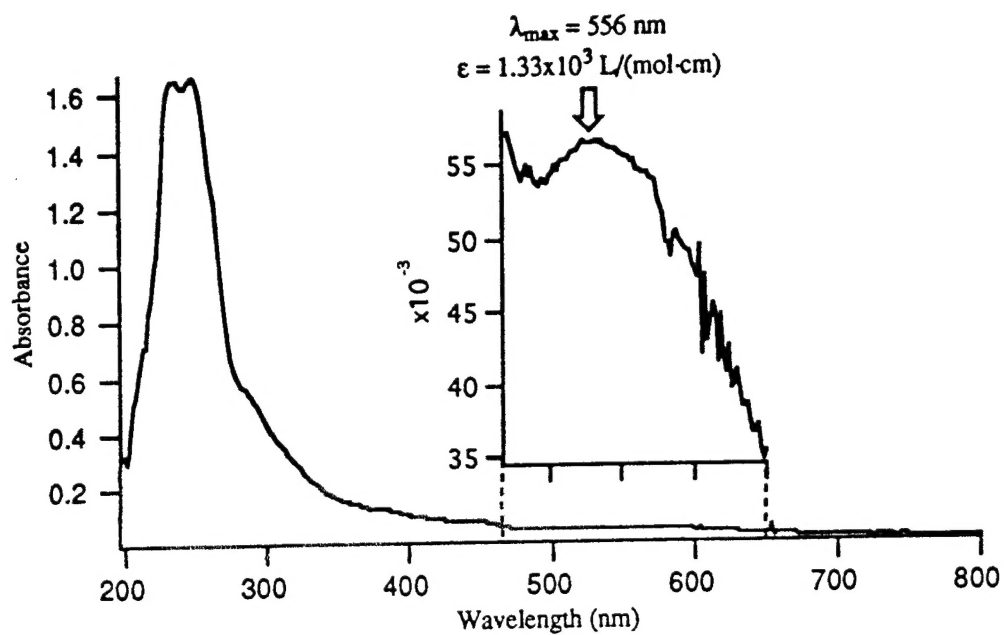
Fig 1

Figure 2
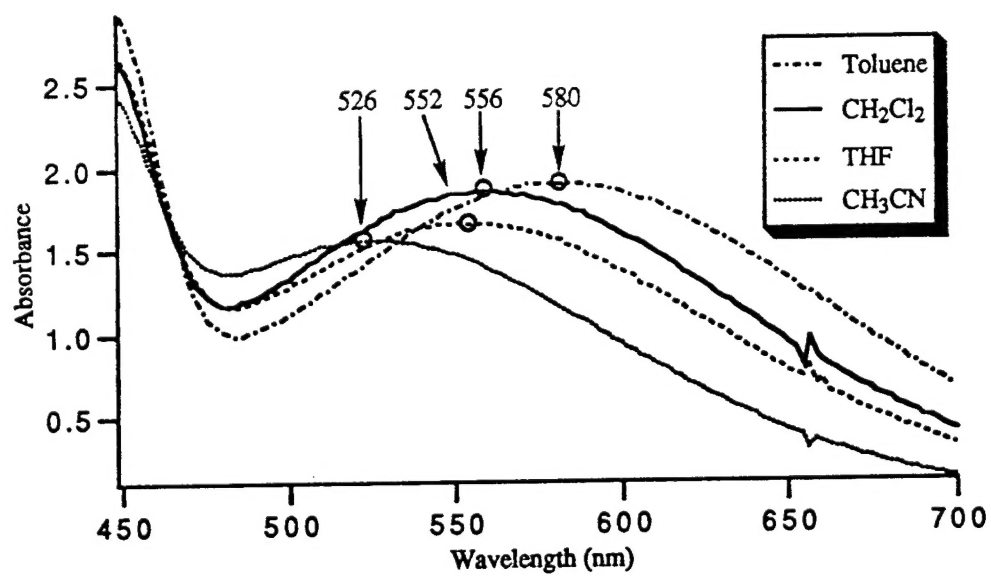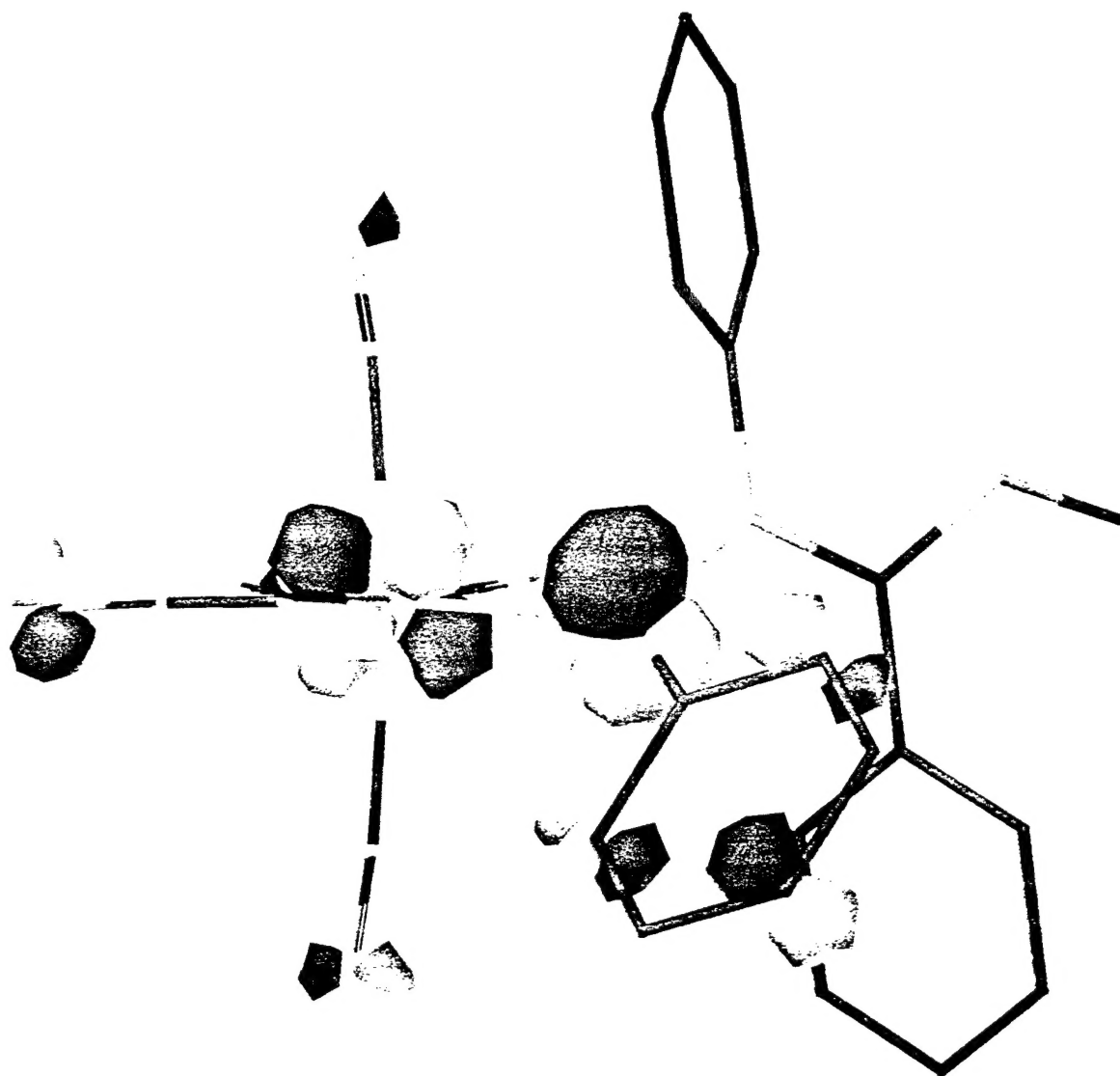
(a)

(b)

Figure 4